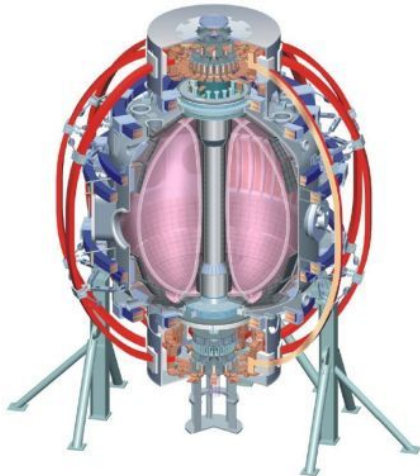


Modeling of Balmer series deuterium spectra with the Cretin code for diagnosing inner divertor re-attachment threshold in NSTX discharges with lithium coatings

Filippo Scotti, PPPL
V. A. Soukhanovskii, H. A. Scott LLNL

APS-DPP Conference 2009
Atlanta, GA



College W&M
 Colorado Sch Mines
 Columbia U
 CompX
 General Atomics
 INEL
 Johns Hopkins U
 LANL
 LLNL
 Lodestar
 MIT
 Nova Photonics
 New York U
 Old Dominion U
 ORNL
 PPPL
 PSI
 Princeton U
 Purdue U
 SNL
 Think Tank, Inc.
 UC Davis
 UC Irvine
 UCLA
 UCSD
 U Colorado
 U Illinois
 U Maryland
 U Rochester
 U Washington
 U Wisconsin

Culham Sci Ctr
 U St. Andrews
 York U
 Chubu U
 Fukui U
 Hiroshima U
 Hyogo U
 Kyoto U
 Kyushu U
 Kyushu Tokai U
 NIFS
 Niigata U
 U Tokyo
 JAEA
 Hebrew U
 Ioffe Inst
 RRC Kurchatov Inst
 TRINITY
 KBSI
 KAIST
 POSTECH
 ASIPP
 ENEA, Frascati
 CEA, Cadarache
 IPP, Jülich
 IPP, Garching
 ASCR, Czech Rep
 U Quebec

Abstract

Application of evaporated lithium coatings on graphite divertor tiles in NSTX led to a reduction of divertor recycling.

The inner divertor electron density and recombination rate were also drastically reduced, suggesting that the normally detached inner divertor re-attached in many lithium-assisted ELM-free H-mode discharges.

This observation was based on the divertor brightness profiles of Stark-broadened ultraviolet spectral lines from the Balmer series $n = 2-7 \dots 12$ transitions.

To understand the divertor transport regimes with reduced recycling and the density thresholds for both the inner divertor detachment and X-point MARFE formation, we are developing a simulation of the NSTX divertor spectra in a realistic viewing geometry using the Cretin code. The non-local thermodynamic equilibrium radiation transport code Cretin uses a 1-D plasma model with neutral diffusion and line shape calculations based on the quasi-static ion microfield approximation and a binary electron impact collision model.

*Work supported by the U.S. DOE under Contracts DE-AC52-07NA27344 and DE-AC02-09CH11466.

Outline & Summary

- Introduction: **NSTX divertor regimes** strongly modified with Lithium deposition.
- **SOL Five Point Model** was used to simulate inner divertor regimes with reduced recycling due to Li coatings:
 - Increase in T_e and reduction in n_e at the target
 - Suggests re-attachment of the inner leg.
- NLTE radiation transport code **CRETIN** was used to simulate Balmer series deuterium spectra in NSTX inner divertor.
- **Stark broadening** from $n=10$ Balmer line was used to estimate n_e in the inner divertor based on:
 - Quasi-static ion microfield approximation
 - Binary electron impact collision model.
- Post Li inner divertor plasmas show **reduced recombination**, **higher T_e** and **reduced n_e** , consistent in both fluid and spectroscopic analysis.

Divertor in STs and NSTX

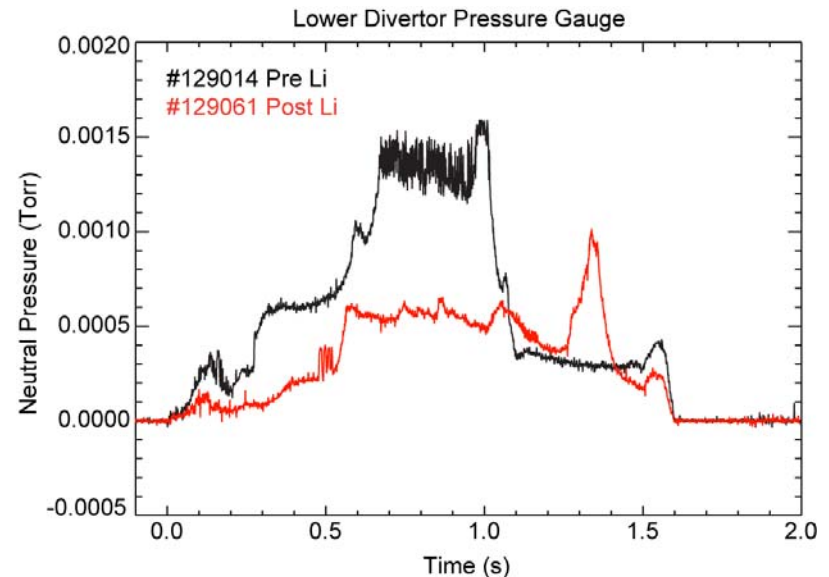
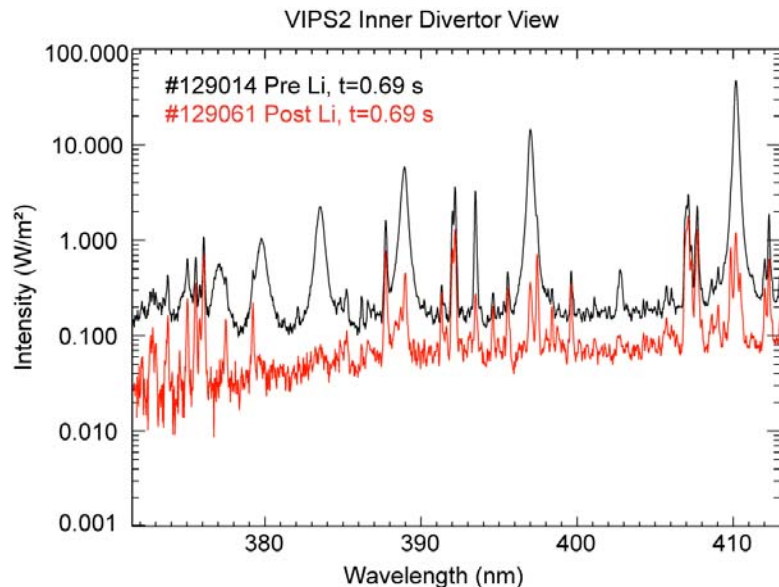
- Spherical Tokamak (ST) Divertor Geometric Features:
 - small surface to volume ratio and plasma wetted area
 - short connection length
 - strong inner/outer heat flux asymmetry
- Achievement of dissipative regimes (radiative/detached) is challenging
BUT
- Potential CTF application: heat/particle fluxes potentially comparable to reactor
- NSTX:
 - Symmetric upper and lower divertor with graphite tiles
 - Open geometry: flexibility in plasma shaping
 - No active pumping: secular core density rise
 - Outer divertor: generally attached, high gas puffing to partially detach
 - Inner divertor detaches early in the discharge ($n_{e-core} > 2-3 \cdot 10^{19} \text{ m}^{-3}$)

Lithium as PFC in NSTX

- Lithium used on NSTX as a PFC: [pellets injection](#) or [evaporative deposition](#) on the divertor plates. Next step in FY2010: Liquid Lithium Divertor module.
- Lithium capability of pumping hydrogen offers a potential solution for density control.
- [Performance improvements](#) in reduced recycling regimes with Li deposition:
 - ELMs suppression,
 - improvement of energy confinement and plasma performance,
 - higher pedestal T_e and T_i (flatter T profile)

Research Motivation: Experimental Observation of Inner Divertor Re-attachment After Li Deposition

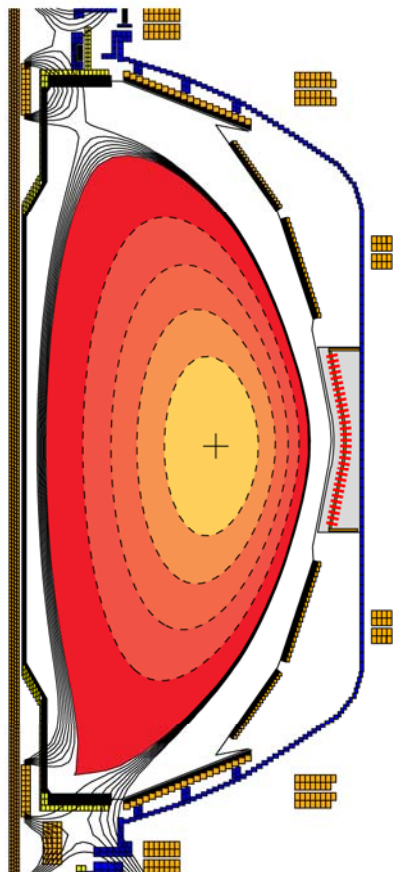
- The reduced recycling strongly modifies the divertor plasma:
 - Reduction/disappearing of high-n Balmer lines
 - Reduced Stark broadening of Balmer lines
 - Reduced neutral pressure
- This suggests that recombination is strongly reduced and inner divertor leg re-attaches in Li-assisted discharges.
- Fluid and spectroscopic modeling can be useful to understand the physics of these divertor regimes.



NSTX Reference Discharges

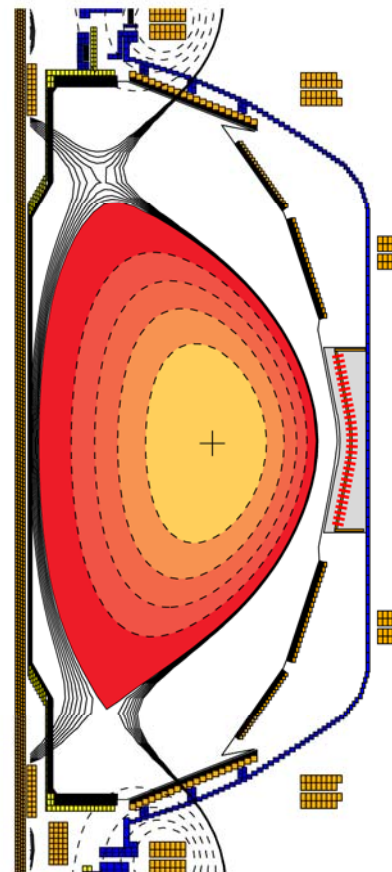
High elongation/ triangularity

Low elongation/ triangularity



shot	129014
time(s)	0.682
κ	2.362
δ	0.376
$\beta_T(\%)$	17.872
β_N	5.175
δR_{sep}	-0.007
$B_T(T)$	0.4
$I_P(MA)$	900
$P_{NBI}(MW)$	6

EFIT02 129014 0.682 s

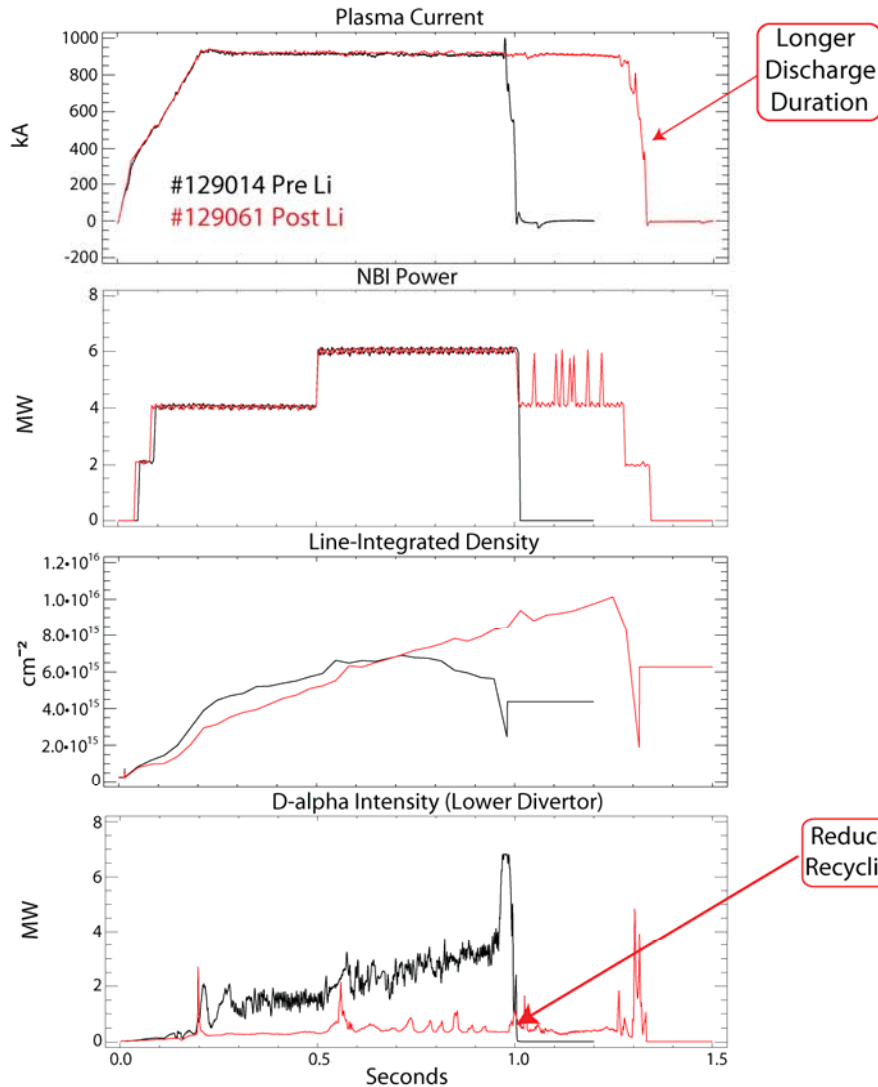


shot	129020
time	0.451
κ	1.829
δ	0.475
$\beta_T(\%)$	11.162
β_N	4.336
δR_{sep}	-0.004
$B_T(T)$	0.45
$I_P(MA)$	800
$P_{NBI}(MW)$	6

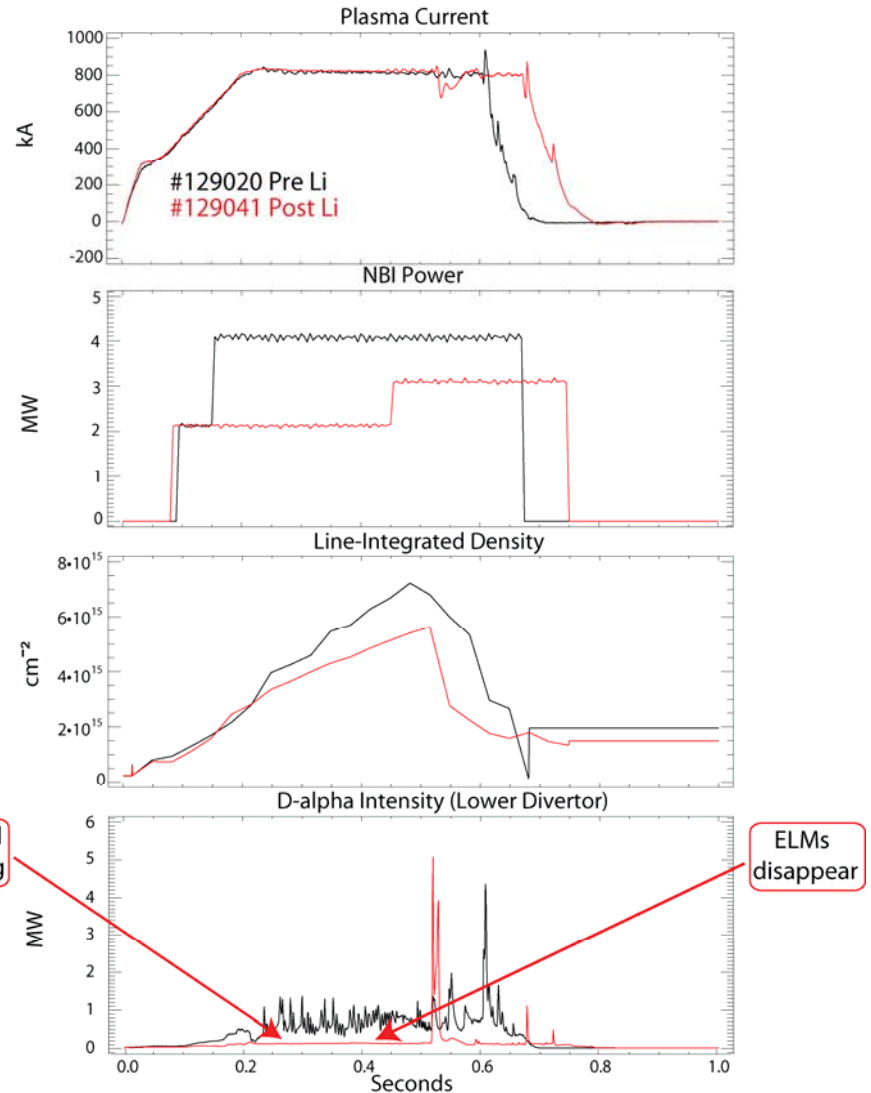
EFIT02 129020 0.451 s

Lithium Coating Increases Discharge Duration, Reduces Recycling and Suppresses ELMs

High elongation/ triangularity



Low elongation/ triangularity



SOL/Divertor Modeling

- SOL plasma transport can be described by the Braginskii equations.
- A simpler set of equations can be used to describe the transport parallel to the magnetic field.

- **Continuity Equation**

$$\frac{\partial(nv)}{\partial x} = n(n_n \langle \sigma v \rangle_i - n \langle \sigma v \rangle_{rec}) + S_{\perp}$$

- **Momentum Equation**

$$\frac{\partial(mnv^2 + 2nT)}{\partial x} = -mnv(n_n \langle \sigma v \rangle_{cx+el} + n \langle \sigma v \rangle_{rec})$$

- **Power Balance Equation**

$$\frac{\partial}{\partial x} \left(-\kappa_0 T^{\frac{5}{2}} + \frac{1}{2} mnv^3 + 5nT v \right) = -n^2 f_Z L_Z - \frac{3}{2} T n n_n \langle \sigma v \rangle_{cx+el} - n E_{ion} \langle \sigma v \rangle_i + Q_{\perp}$$

Five point model of the SOL plasma

- Simplified 2-point/1-D models useful to understand divertor detachment.
- In this work a **five point model** based on [R. Goswami, *Phys. Plasmas*, **8**,3 (2001).], was used.
- Simplified continuity, momentum and power equations are solved for the electrons in five different regions from the midplane to the divertor target.
- **Radiation**, **ionization**, **momentum loss** and **volume recombination** effects are included in the model assuming constant rates.
- Analytical solution in the five regions provides a pseudo 1-D profile of plasma parameters, n , T , v and pressure.

Five point model of the SOL plasma

- Region 1: volumetric SOL heat Q_{\perp} and particle sources S_{\perp} , from midplane ($x=0$) to X-point ($x=x_x$).

$$\frac{d}{dx}(nv) = S_{\perp}, \quad \frac{dp}{dx} = 0, \quad \frac{d}{dx} \left(\kappa_0 T^{\frac{5}{2}} \frac{dT}{dx} \right) = -Q_{\perp}$$

- Region 2: Conduction region, until start of energy loss zone ($x=x_L, T(x_L)=10\text{eV}$).

$$\frac{d}{dx}(nv) = 0, \quad \frac{dp}{dx} = 0, \quad \frac{d}{dx} \left(\kappa_0 T^{\frac{5}{2}} \frac{dT}{dx} \right) = 0$$

- Region 3: Radiation front region (max. C radiation eff.) until start of the neutral zone ($x=x_C, T(x_C)=4\text{eV}$).

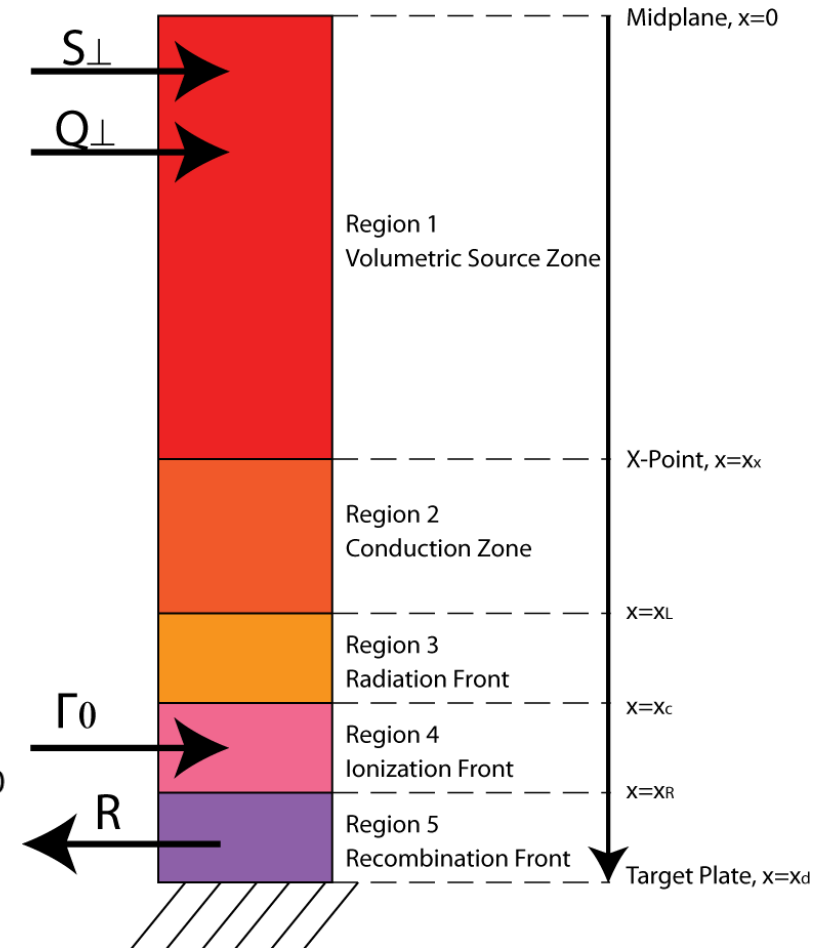
$$\frac{d}{dx}(nv) = 0, \quad \frac{dp}{dx} = 0, \quad \frac{d}{dx} \left(\kappa_0 T^{\frac{5}{2}} \frac{dT}{dx} \right) = L$$

- Region 4: Ionization front region (most neutrals are ionized) until onset of recombination region ($x=x_R, T(x_R)=1.6\text{eV}$).

$$\frac{d}{dx}(nv) = \Gamma_0 \delta(x - x_C), \quad \frac{dp}{dx} = -m_i v_x nv, \quad \frac{d}{dx} \left(\kappa_0 T^{\frac{5}{2}} \frac{dT}{dx} \right) = 0$$

- Region 5: Recombination front region (recombination exceeds ionization), until divertor plate.

$$\frac{d}{dx}(nv) = -R, \quad \frac{dp}{dx} = -m_i v_x nv, \quad \frac{d}{dx} \left(\kappa_0 T^{\frac{5}{2}} \frac{dT}{dx} \right) = 0$$



Modeling Reduced Recycling in Lithium-assisted Discharges

- Volumetric heat source Q_{\perp} obtained from estimates of the power to the SOL
- Ionization fluxes to the center stack Langmuir probes were used to estimate the scaling of the volumetric particle source S_{\perp}
- Reduced recycling is modeled decreasing the amplification factor Γ of the ionization flux in the divertor region due to the reduced neutral pressure
- The charge exchange frequencies ν are also modified accordingly.
- Different simulation scenarios:

- In Scenario-1 $f_{RAD} = \frac{L \cdot \delta_L}{q_{\parallel}}$ is kept constant for Pre/Post Li discharges

- In Scenario-2 f_{RAD} is increased for Pre-Li discharges and decreased for Post-Li discharges

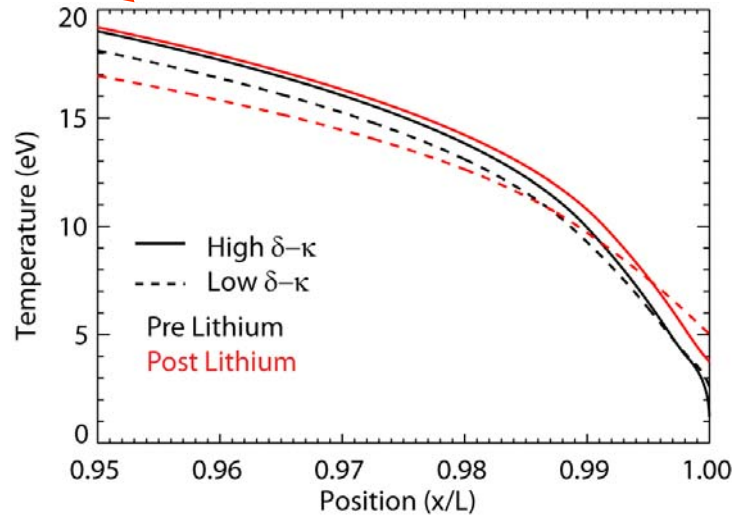
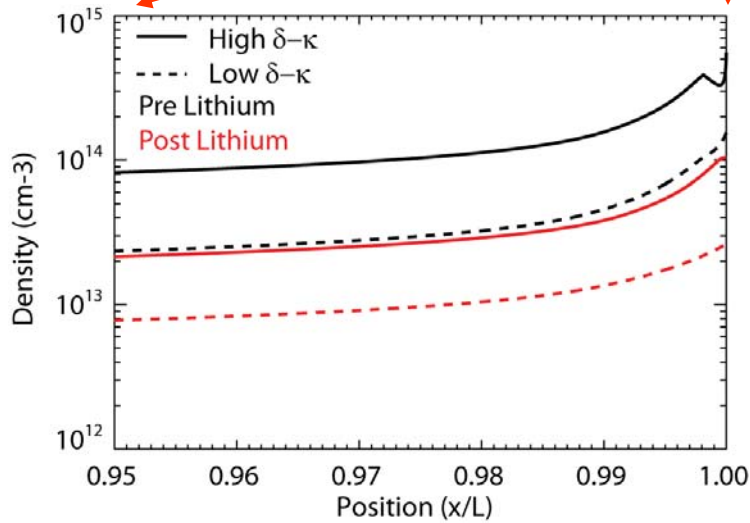
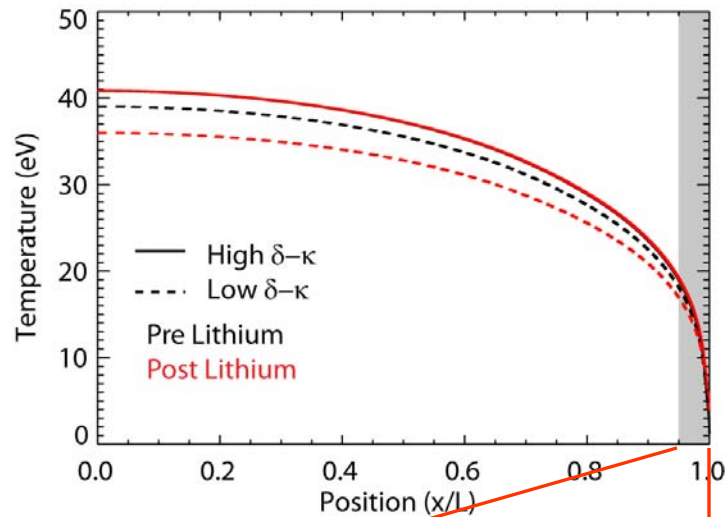
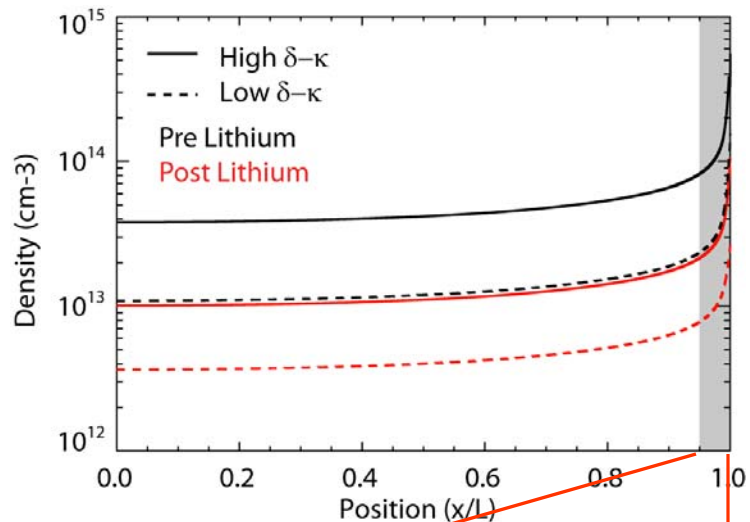
Five Point Model: 1st Scenario

	High δ - κ , Pre-Li	High δ - κ , Post-Li	Low δ - κ , Pre-Li	Low δ - κ , Post-Li
Q_{\perp} (MWm ⁻³)	3.28	3.28	2.8	2.1
S_{\perp} (10 ²³ s ⁻¹ m ⁻³)	2.5	1.2	1.8	0.8
Γ_0 (10 ²³ s ⁻¹ m ⁻²)	20	3.2	1.1	0.05
V_0 (10 ⁵ S ⁻¹)	4	1.33	0.26	0.026
R (10 ²³ s ⁻¹ m ⁻³)	1	1*	1	1*

- Midplane-target connection length $L=13\text{m}$, Xpoint-Target $L_x=4\text{m}$
- Radiated power fraction was kept constant in the 4 different simulations.
- *In Lithium discharges the higher T_e at the target places the divertor in a regime of low radiation and no recombination.

Simulation Results (1st Scenario)

Re-attachment of Inner Divertor in Lithium Discharges



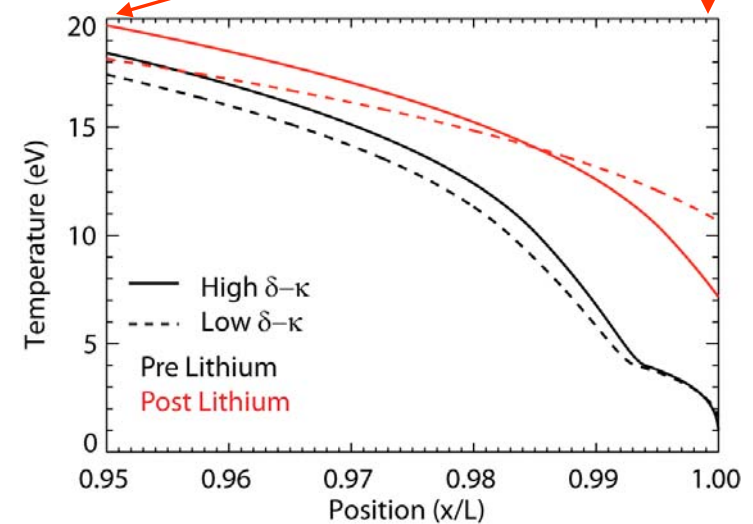
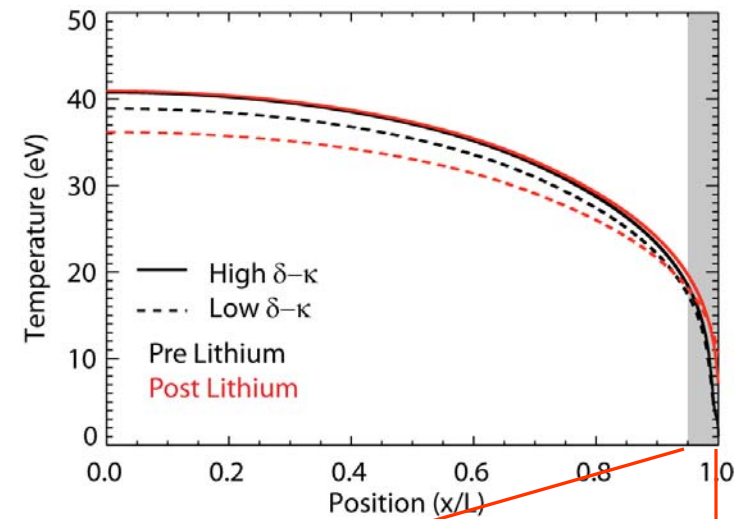
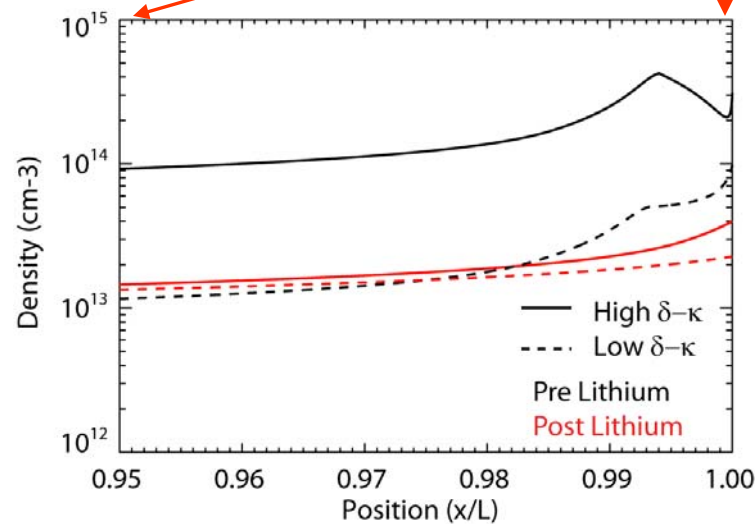
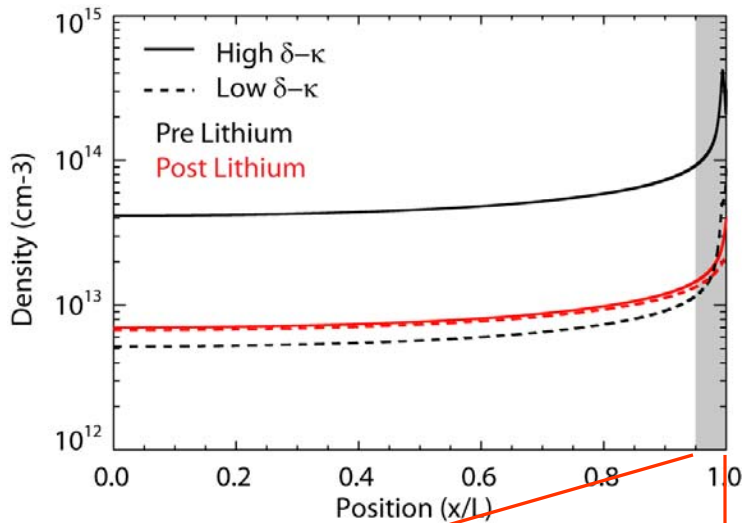
Five Point Model: 2nd Scenario

Varying f_{RAD}

	High δ - κ , Pre-Li	High δ - κ , Post-Li	Low δ - κ , Pre-Li	Low δ - κ , Post-Li
Q_{\perp} (MWm^{-3})	3.28	3.28	2.8	2.1
S_{\perp} ($10^{23} \text{ s}^{-1}\text{m}^{-3}$)	1.25	1.2	0.9	0.8
Γ_0 ($10^{23} \text{ s}^{-1}\text{m}^{-2}$)	10	3.2	0.55	0.05
V_0 (10^5 S^{-1})	4	1.33	0.26	0.026
R ($10^{23} \text{ s}^{-1}\text{m}^{-3}$)	1	1*	1	1*

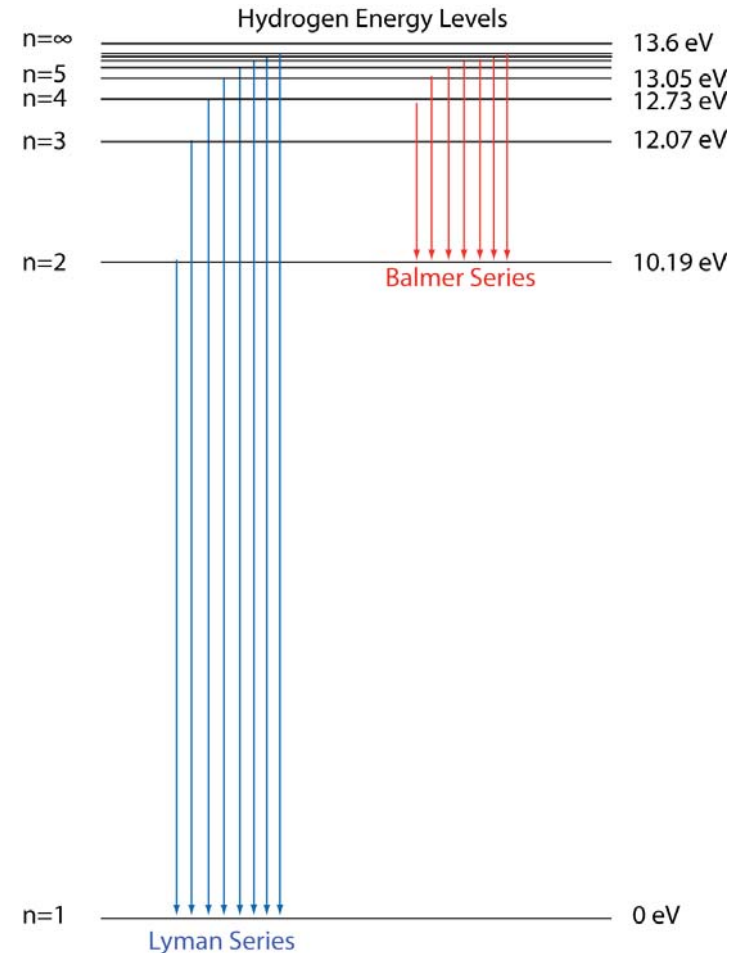
- A 5-10% increase in the radiated power for the pre lithium discharges allowed the accessibility of the detached regime for lower ionization fluxes (50% in this simulation).
- The recombining, low temperature region expands towards the X-point.
- A reduction of the radiated power fraction for the post Li case increases T_e at the divertor target (even 50% higher fluxes would still allow an attached solution).

Simulation Results (2nd Scenario) Te at Target Increases for Reduced f_{RAD}



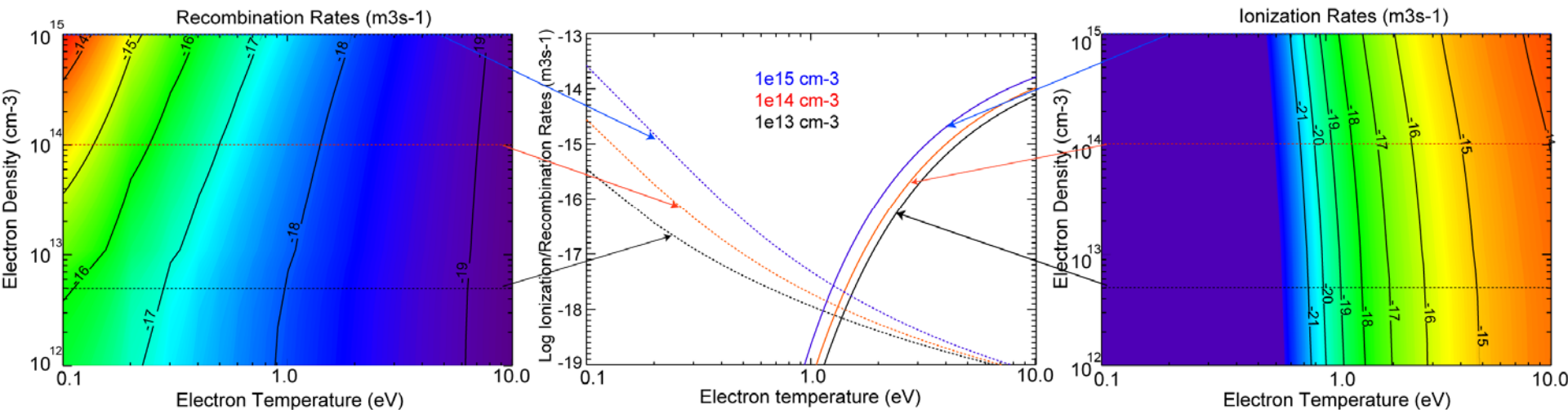
CRETIN Code: Atomic Model

- **CRETIN** is a non-local thermodynamic equilibrium (NLTE) radiation transport code, [H. A. Scott, *J. Quant. Spectrosc. and Radiat. Transfer*, **71** (2001)].
- A simple Hydrogenic model for Deuterium (D) levels was used to generate the atomic structure.
 - Principal quantum numbers up to $n=30$ and orbital quantum numbers up to $l=14$ were included.
 - No molecular species/transitions are included.
- **CRETIN** can be run as postprocessor to external data (plasma parameters, e.g. n , T) or it can generate its own time-space dependent profiles.
 - 1-D steady state plasma models were used in this work.



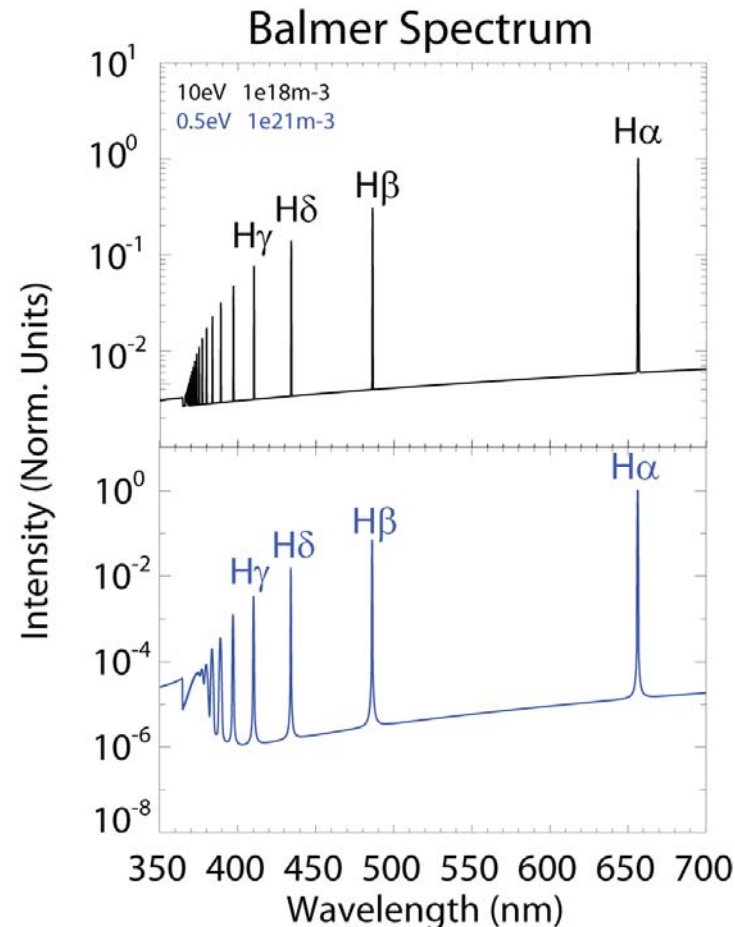
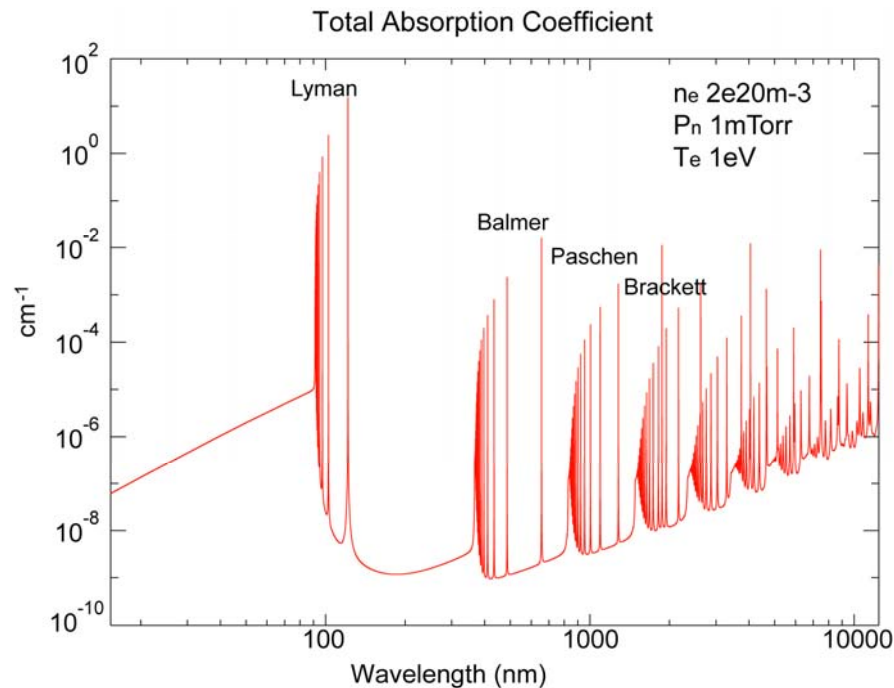
CRETIN Code Reaction Rates

- **CRETIN** calculates rates for ionization, excitation and recombination (collisional and radiative) based on local parameters.
 - The spatial coupling occurs through radiation transport.
 - Atomic populations are then derived.
 - Continuum and line radiation are treated separately and coupled to the atomic kinetics.
- Rates calculated by **CRETIN** based on an Hydrogenic model for Deuterium, show that for low T_e (<1.5 eV) and high n_e ($>1e13\text{cm}^{-3}$), recombination dominates over ionization processes.



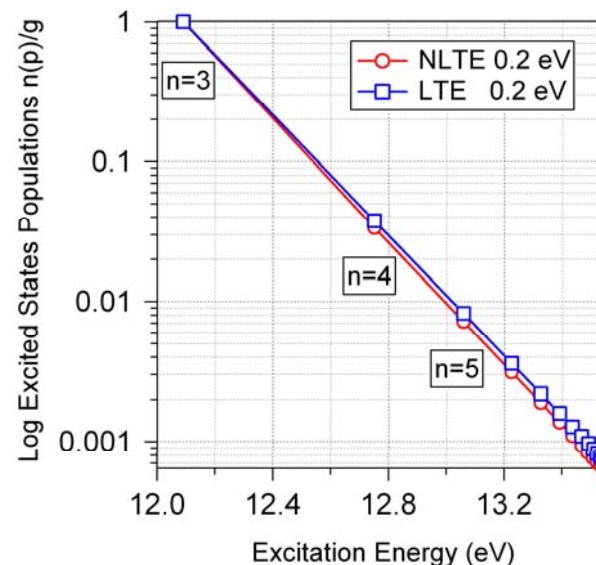
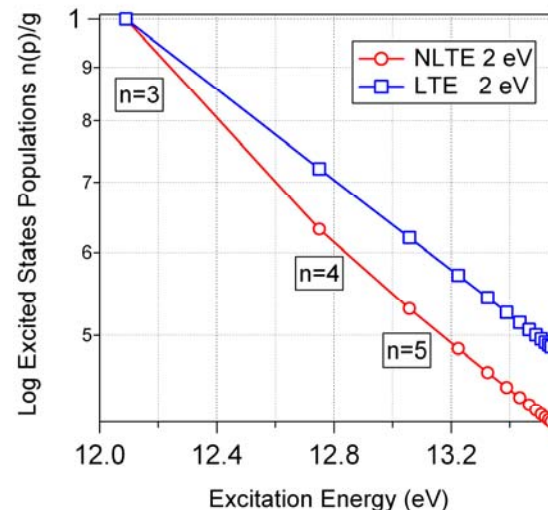
Recombination Processes in the Divertor Region

- Due to recombination processes high- n excited states are efficiently populated. Their relaxation results in the appearance of the high- n UV Balmer lines spectra.
- In high n_e low T_e plasmas, radiation trapping could modify the excited states level populations. Balmer series lines radiation can be assumed optically thin.



High-n Balmer transitions as plasma diagnostics

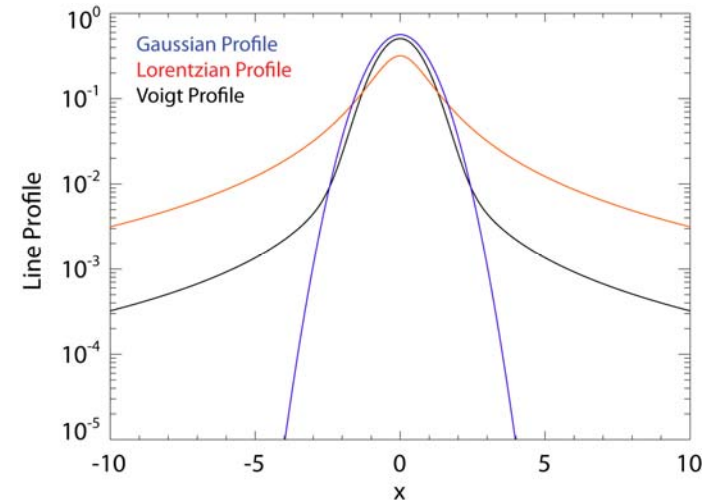
- Signature of recombination.
- For $T_e < 1.5$ eV, T_e diagnostics:
 - From the slope of the excited states population against the level energy (need assumptions of Saha-Boltzmann equilibrium).
 - From the relative intensity of line and continuum background. (neglect molecular pseudo-continuum background).
 - From the slope of photo-recombination continuum.
- Stark broadening of Balmer lines as an electron density diagnostics.



Stark Broadening and Line Shape Calculations

- Broadening mechanisms:

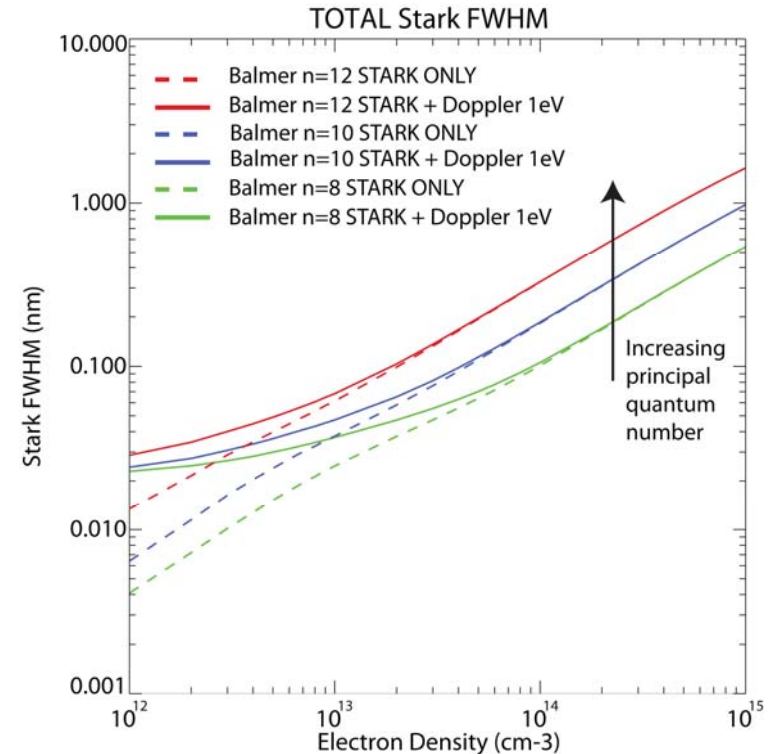
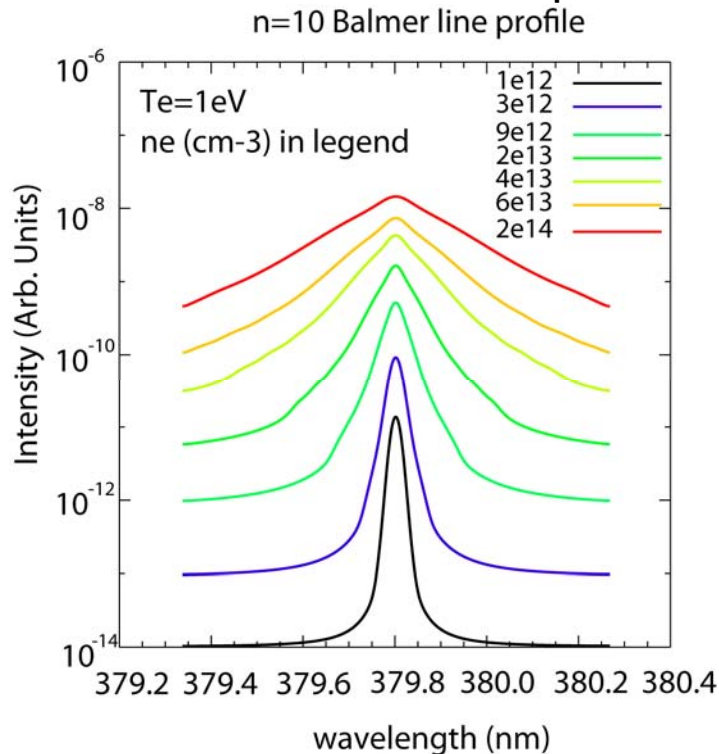
- Natural broadening (Lorentzian)
- Doppler broadening (Gaussian) → Voigt Profile
- Stark broadening (Lorentzian)



- Stark effect generated by the action on the neutral emitter of the electric microfield created by the perturber particles at scales where quasi neutrality is not fulfilled.
- **CRETIN** includes a code for line shape calculations, **TOTAL** [Calisti, PRA 1990].
- **TOTAL**: line shapes from [binary electron impact model](#) and [quasistatic ion microfield](#).
- Electrons: binary (one perturber /collision) and instantaneous impact approximations.
- Ion quasistatic approx: collisions as an almost constant perturbation. Requires line width much larger than typical fluctuation frequency of ion microfield.

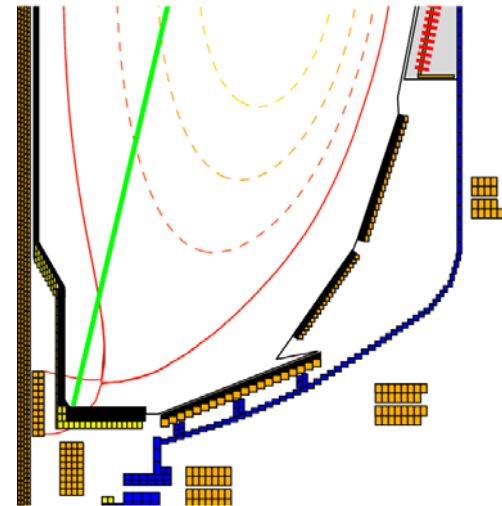
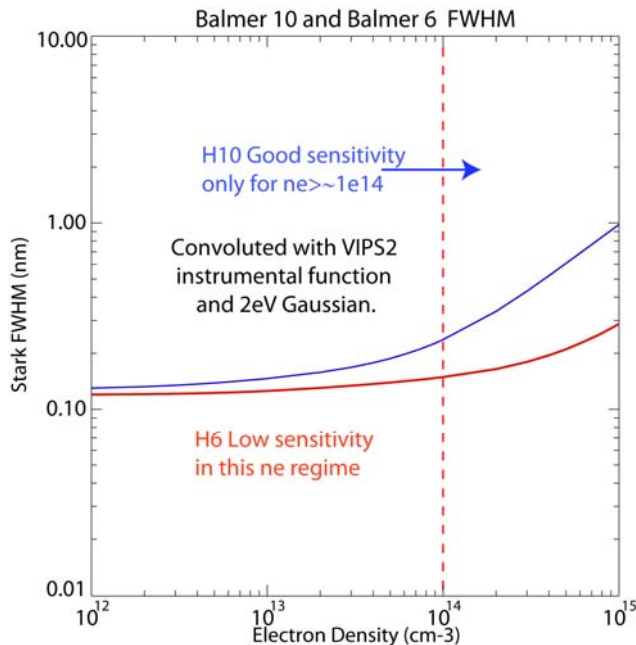
Stark Broadening and Line Shape Calculations

- Stark broadening increases with n_e due to the higher microfields.
- **High-n level transitions** show larger broadening. More suitable as n_e diagnostics.
- In the present work, Deuterium UV Balmer series lines with n_{\max} up to 15 were treated with **TOTAL** to take into account for Stark effect and Doppler broadening.
- The Gaussian instrumental response was convolved with the line shape generated by **TOTAL** to obtain the final spectra.



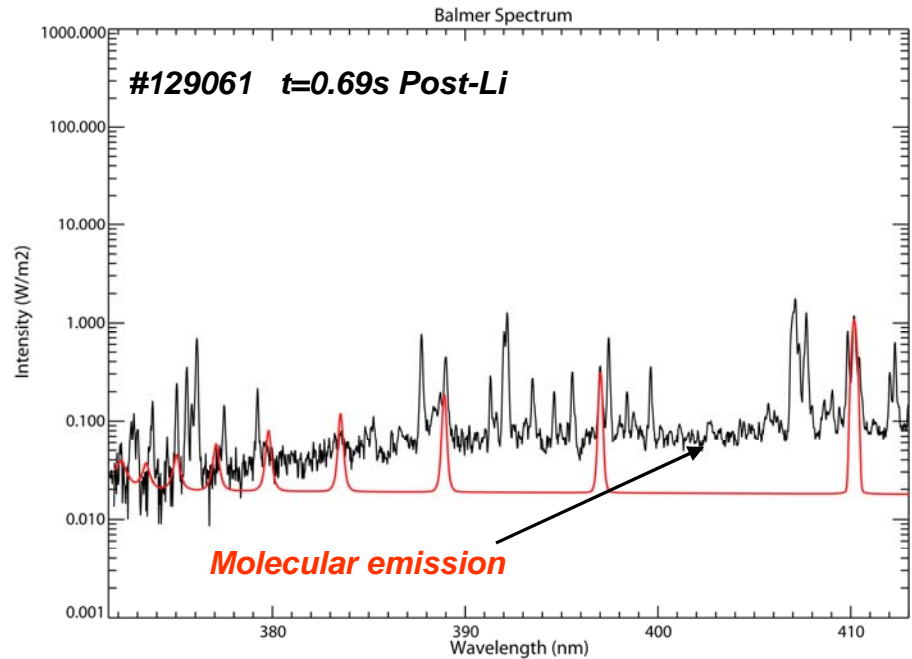
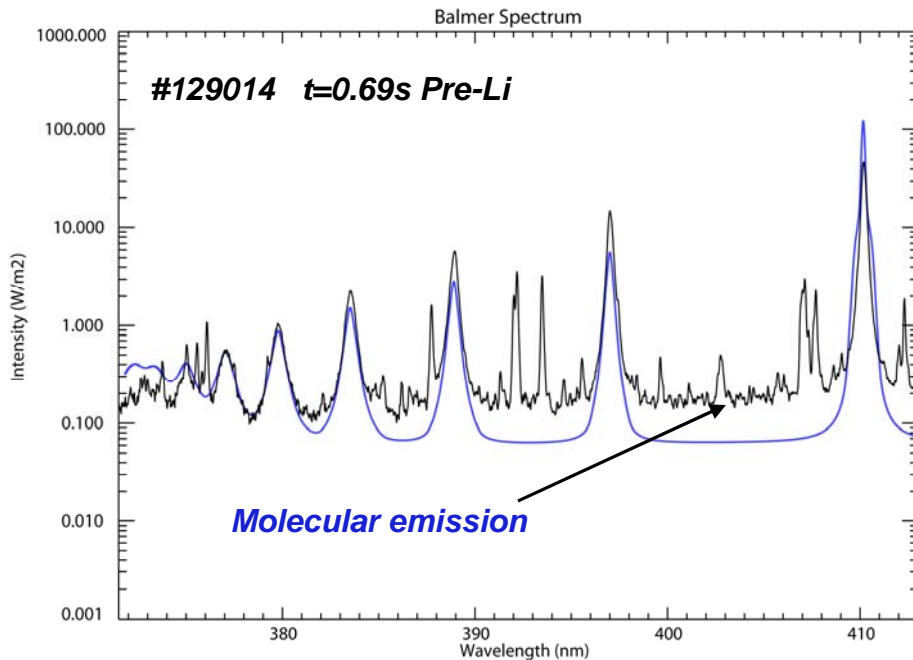
CRETIN Simulation

- Data were acquired by the divertor spectrometer VIPS:
 - Viewing chord looking at the inner divertor
 - Instrumental function 1.1 Å (1.2 Å after convolution with 2eV ions).
- n_e was estimated from Balmer line Stark broadening from $n=10$.
- 1D CRETIN simulations were used to reproduce spectroscopic data.
- Simulated spectra were scaled by a constant factor in order to reproduce the detector view.



1-D CRETIN Simulation

High elongation/ triangularity



$n_e \sim 5 \pm 0.5 \times 10^{20} \text{ m}^{-3}$ from H10 Stark Broadening

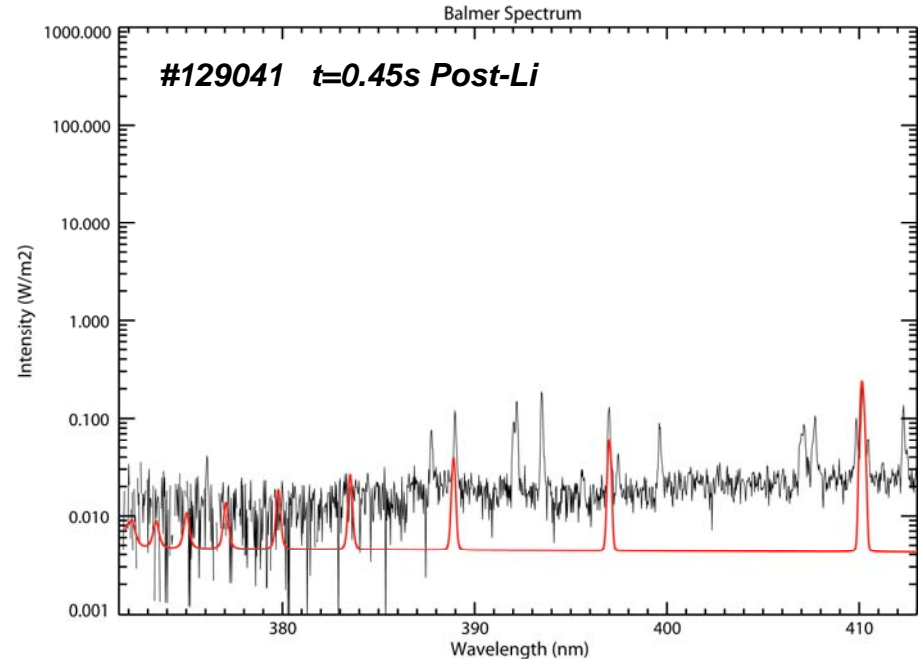
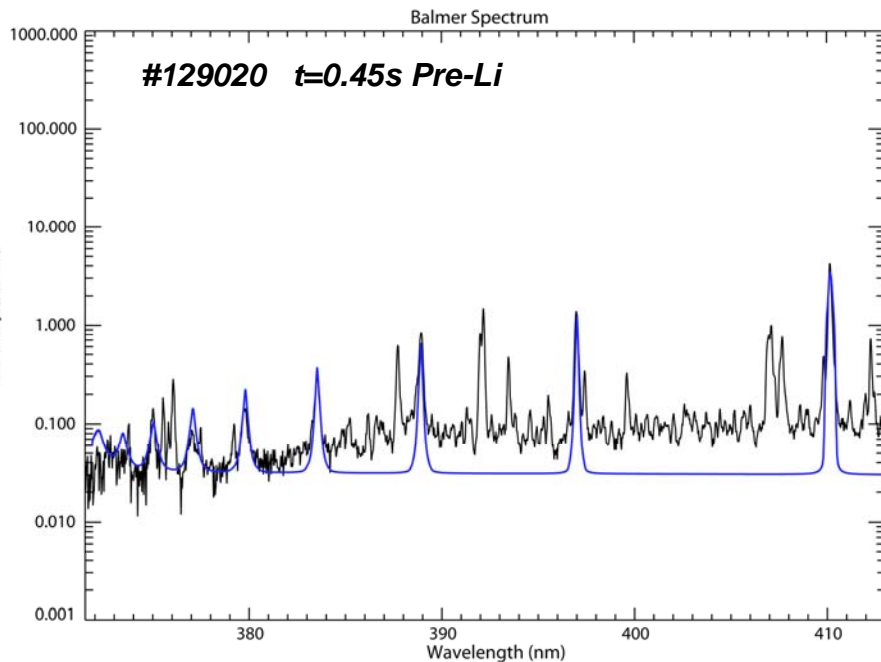
$T_e \sim 1.1 \text{ eV}$

$n_e = 1.1 \pm 0.2 \times 10^{20} \text{ m}^{-3}$ from H6 Stark Broadening

Example spectrum for $T_e = 5 \text{ eV}$ is shown in red

1-D CRETIN Simulation

Low elongation/ triangularity

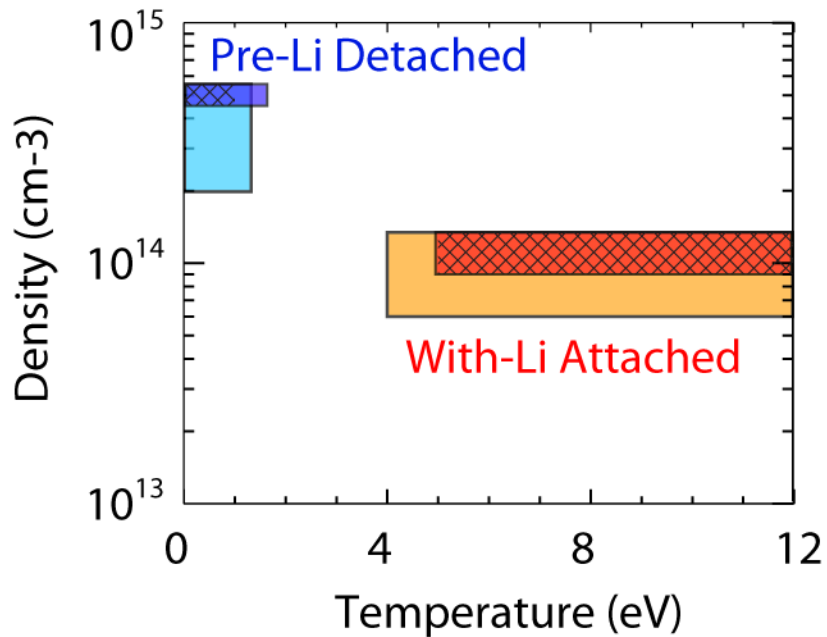


$n_e \sim 1.3 \pm 0.2 \times 10^{20} \text{ m}^{-3}$ from H10 Stark Broadening
 $T_e \sim 3 \text{ eV}$

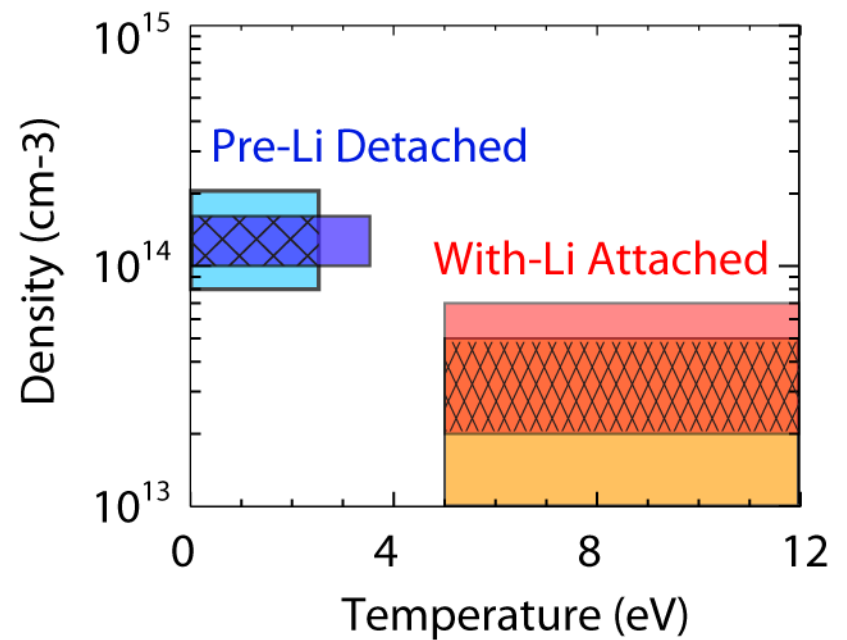
$N_e \sim 5 \pm 3 \times 10^{19} \text{ m}^{-3}$ from H6 Stark broadening
Example spectrum for $T_e = 7 \text{ eV}$ is shown in red

Results Comparison

High elongation



Low elongation



5 Point Model 5 Point Model
Spectroscopy Spectroscopy

Discussion

- Five Point Model:
 - Helps to qualitatively explain the lower recycling regimes but
 - Constant rates are used for the atomic processes
 - Perpendicular transport effects are ignored in this treatment
 - Radiation losses are overestimated
- Sensitivity
 - H10 Stark broadening is only sensitive to high densities ($n > 1e14 \text{cm}^{-3}$)
 - Higher-n transitions would be more convenient but intensity is too low (in attached case only H6 is available)
- Contamination issues:
 - Carbon impurity lines make difficult excited state population evaluation especially in the lower density attached regimes.
 - Molecular emission significantly modifies the continuum background